Graphical Analysis of Mass and Anisotropy Changes Observed by Plasmon-Waveguide Resonance Spectroscopy Can Provide Useful Insights into Membrane Protein Function

Zdzislaw Salamon and Gordon Tollin
Department of Biochemistry and Molecular Biophysics, University of Arizona, Tucson, Arizona

ABSTRACT Plasmon-waveguide resonance spectroscopy is a recently developed optical method that allows characterization of mass and structural changes in two-dimensionally ordered thin films (e.g., proteolipid membranes) deposited onto a sensor surface. Full analysis of these systems involves fitting theoretical curves (obtained using Maxwell's equations) to experimental spectra measured using *s*- and *p*-polarized excitation. This allows values to be obtained for refractive indices and optical extinction coefficients in these two directions, as well as a value for film thickness, thereby providing information about mass density and anisotropy changes. This is a time-consuming process that works well for simple systems in which only a single conformational event occurs, but cannot distinguish between events involving multiple conformations that proceed either sequentially or in a parallel series of events. This article describes a graphical method that can distinguish between mass density and anisotropy changes in a simpler, more rapid procedure, even for processes that proceed via multiple conformational events. This involves measurement of plasmon-waveguide resonance spectral shifts obtained upon molecular interactions occurring in deposited films with both *s*- and *p*-polarized excitation, and transforming these from an (*s*-*p*) coordinate system into a (mass-structure) coordinate system. This procedure is illustrated by data obtained upon the binding of a small peptide, penetratin, to solid-supported lipid bilayer membranes.

INTRODUCTION

Plasmon-waveguide resonance (PWR, or as originally called in Salamon et al., 1997, coupled plasmon-waveguide resonance or CPWR) spectroscopy is an optical technique for probing events occurring at surfaces and interfaces (Salamon and Tollin, 1999a,b). It is based upon the coupling of plasmons (charge density oscillations) excited by light in thin metal films, with waveguide modes in a dielectric layer overcoating the metal film. The coupling generates a surface-localized (evanescent) electromagnetic wave that propagates along the outer surface of the dielectric layer. The electric field intensity of this surface-bound electromagnetic wave, which can be excited by both *p*- and *s*-polarized light, decays exponentially with distance from the interface between the surface of the dielectric layer and the emergent medium (Salamon et al., 1999; Salamon and Tollin, 2001a, 1999a,b). Such an evanescent wave can be employed to characterize the structural properties of molecular assemblies deposited onto the dielectric surface that are organized as two-dimensional systems (Salamon et al., 2003, 2000a, 1999; Salamon and Tollin, 2001b, 2000).

It is well recognized that monolayer assemblies of molecules at surfaces and interfaces can display long-range order. This important structural characteristic is one of the fundamental attributes that control physicochemical processes occurring within such systems. Biological membranes are an important example of such ordered two-dimensional arrays. These are self-assembling proteolipid aggregates consisting of a lipid bilayer associated with a variety of integral (transmembrane) and peripheral (surface-bound) proteins. An additional important characteristic of the two-dimensional organization of biomembranes is their fluid and dynamic nature. Both the organization and the dynamics of biological membranes are essential in functional activity, during which the membrane structural organization undergoes significant changes as a result of interactions between lipid and protein molecules. Thus, experimental techniques employed to study such complex anisotropic and dynamic structures must be capable of assessing these characteristics. As has been demonstrated in earlier publications, one such recently developed methodology is coupled plasmon-waveguide resonance (Salamon et al., 1997; Salamon and Tollin, 1999a,b), which, combined with techniques for forming solid-supported proteolipid membranes, provides a powerful tool for kinetic, thermodynamic, and structural studies of biomembranes (Salamon et al., 1993, 1994, 2000b). In this article, we present a new method for analyzing PWR spectra that has many advantages over presently existing analysis protocols, especially for biological systems.

Submitted September 3, 2003, and accepted for publication November 10, 2003.

Address reprint requests to Gordon Tollin, Dept. of Biochemistry and Molecular Biophysics, University of Arizona, Tucson, AZ 85721. Tel.: 520-621-3447; Fax: 520-621-9288; E-mail: gtollin@u.arizona.edu.

© 2004 by the Biophysical Society

0006-3495/04/04/2508/09 $2.00

PWR spectroscopy

Detailed descriptions of the PWR technology, including both experimental and theoretical aspects, have been presented elsewhere (Salamon and Tollin, 1999a,b; 2000). Here we will discuss those topics that are especially important in the context of this work. PWR spectroscopy is based on the

measurement of reflected light intensity, using a relatively simple optical detection system whose geometrical arrangement permits a complete isolation of the optical probe from the system under investigation. This allows studies to be carried out on complex heterogeneous mixtures. A PWR resonator typically consists of a prism that is coated by a thin metal film (usually silver or gold), overcoated by a layer of a dielectric material (usually silica) functioning as a waveguide. Electronic oscillations (plasmons) in the metal film can be resonantly excited by *p*-polarized light (i.e., linearly polarized light with the electric vector perpendicular to the surface plane). These generate a surface-localized evanescent electromagnetic field that can probe the optical properties perpendicular to the film plane of materials immobilized at the surface, and that can couple with waveguide modes within the dielectric coating. The waveguide modes can also be excited by *s*-polarized light (i.e., the electric vector parallel to the surface plane) and can thus probe the optical properties of immobilized materials parallel to the surface plane. Therefore, PWR spectroscopy can characterize the anisotropic optical properties of ordered materials deposited onto the resonator, e.g., a proteolipid membrane. Maxwell's equations provide an analytical relationship between these optical properties and the *p*- and *s*-polarized PWR spectra, allowing their evaluation. Plasmon excitation occurs under resonance conditions when the energy and momentum of the incident photons and the surface plasmons are matched (Salamon et al., 1999; Salamon and Tollin, 2001a). This condition can be fulfilled by changing the incident angle of the exciting light at a constant value of photon energy (Salamon et al., 1999; Salamon and Tollin, 1999a,b). The resulting variation in reflected light intensity constitutes a PWR spectrum. Furthermore, any alteration in the optical properties at the surface of the resonator will affect the resonance conditions and therefore change the resonance spectrum.

The optical properties of the resonator and immobilized molecules can be fully described by the complex dielectric constant that contains the refractive index (n) and the extinction coefficient (k) at the excitation wavelength. The shape of the PWR spectrum, described by its halfwidth (i.e., the width of the spectrum measured at half-depth), by the depth of the spectrum and by its angular position, are determined by these optical parameters as well as by the thickness (t) of the interfacial layer, all of which can be evaluated by using Maxwell's equations (Salamon et al., 1997a, 1999; Salamon and Tollin, 1999a,b, 2001a). The fact that there are three measured spectral parameters and three optical parameters describing the properties of the interface allows a unique determination of the *n*-, *k*-, and *t*-values by fitting a theoretical resonance curve to the experimental one (Salamon et al., 1997a, 1999; Salamon and Tollin, 1999a,b, 2001a). Inasmuch as the excitation wavelength (632.8 nm) in the experiments described here is far removed from the absorption bands of the lipids and peptide used, a *k*-value other than zero reflects a decrease in reflected light intensity due only to scattering of the evanescent wave by imperfections in the proteolipid film. This effect will not be discussed further in this work.

Although such an approach to analysis of experimental data works well in most cases, there are instances where another approach would be of value. For example, there are situations in which rapid conclusions about the processes occurring within the thin films are required. Although the fitting procedure is certainly the most accurate way of analyzing data, it requires considerable time and effort and therefore appreciably slows the process of reaching such conclusions. A second example is when more than one process takes place within a complex heterogeneous film, resulting in a final spectrum that represents a mixed population. In such a case, fitting the spectrum will yield the average optical parameters and thickness of the film without providing much insight into the processes or species that generate the spectrum. In these situations, an alternative approach can be used that is based upon the following considerations. As has been discussed elsewhere (Salamon and Tollin, 2001b), the refractive index reflects the mass density of material. However, mass is a typical scalar quantity and therefore its value will not depend on the polarization of the exciting light that is used to measure it. On the other hand, refractive index has a directional dependency in the anisotropic proteolipid systems we are dealing with here. This effect has been termed birefringence, i.e., different refractive index values obtained with different polarizations (Salamon and Tollin, 2001b). In general, birefringence results from a molecular shape-dependent polarizability tensor and an internal order in which the asymmetric molecules comprising the film are organized at the interface. Such a microstructure can be thought of as defining a spatial distribution of mass, reflecting the long-range orientation of molecules, their polarizability, and their shape (Salamon and Tollin, 2001b). Therefore, to characterize optically anisotropic biological membranes (or any other anisotropic system) one must define both the average mass density and the spatial mass distribution (i.e., the directional differences in mass density) resulting from the membrane microstructure. Note that isotropic systems will not have such differences in spatial mass distribution, i.e., mass density will be constant over all directions. The characterization of mass density and optical anisotropy is accomplished in PWR spectroscopy by measurements of refractive indices with polarized light. Once these indices are obtained, the average mass density can be described by the square of the average value of the *p*- and *s*-polarized refractive indices, which is related to the total mass by the Lorentz-Lorenz relation (Salamon and Tollin, 2001b). The spatial mass distribution can be described by the refractive index anisotropy, which is proportional to the difference between the *p*- and *s*-polarized refractive indices (Salamon and Tollin, 2001b).

It is important to realize that it is possible to change one of these two quantities without altering the other, e.g., the

average mass density can remain constant, whereas the mass distribution can change as a consequence of alterations in the microstructure of the system (e.g., by changes in conformation or molecular orientation), or vice versa. It is also important to point out that for the average value of the refractive index (and thus the mass) to remain constant, the *p*- and *s*-polarized indices must change by equal amounts in the opposite direction; i.e., if one increases, the other must decrease. Note that the observed PWR spectral shifts will change by the same amount only if the mass sensitivities of the *p*- and *s*-polarizations are equal. If not, differences in sensitivity must be taken into account (see next section). Furthermore, this directional effect would not occur with isotropic systems. On the other hand, if microstructure is unchanged (i.e., if the difference between refractive indices obtained with *p*- and *s*-polarizations remains unaltered, which can occur for both isotropic and anisotropic systems) but mass changes, then both polarized indices must be altered by the same amounts in the same direction (either increasing or decreasing). Again, shifts by the same amount will occur only if the sensitivity of *p*- and *s*-polarizations are equal. These relationships outline the fundamental basis for the simpler and more rapid graphical analysis procedure that is discussed below. The goal of such analysis will be to separate the effects on the PWR spectrum that result from changes in average mass density from those produced by changes in structure, and to obtain such a separation individually for all processes that lead to these changes. This procedure will be illustrated using experimental data previously obtained with a lipid bilayer interacting with the small cell-penetrating peptide penetratin (Salamon et al., 2003).

Principles of graphical analysis of PWR data

The graphical analysis procedure described in this work is based on the following considerations. PWR spectra are determined by both the total mass deposited per unit surface area of the resonator (i.e., average surface mass density) and the spatial distribution of that mass within the system that results from the structure of the deposited film. Although there are three experimental parameters of the resonance spectrum (position, width, and depth) that reflect optical changes occurring in a sample, each of these parameters has a different sensitivity to changes resulting from either mass or structure. In principle, any of them could be considered in a graphical procedure; however, from a practical point of view, the position of the spectrum is the best in which mass (Δ_m) and structural (Δ_{str}) changes are described by *p*- (Δp) and *s*- (Δs) polarized spectral shifts, given by $(\Delta_m) = f_1\,(\Delta p; \Delta s)$, and $(\Delta_{str}) = f_2\,(\Delta p; \Delta s)$.

The separation of mass changes from those due to structure is achieved by transforming the measured spectral changes (i.e., changes in the position of the spectra obtained either with *p*- or *s*-polarized exciting light) from an (*s*-*p*) orthogonal coordinate system into a (mass-structure) one. To perform such a transformation one must be able to place mass and structural axes within the original (*s*-*p*) coordinate system. This can be done if one knows the following two properties of the sensor/measured system:

1. The mass sensitivity of the *p*- and *s*-axes in the (*s*-*p*) coordinate system, i.e., the sensor must be calibrated either experimentally or theoretically to find out how much shift a unit isotropic mass causes to both *p*- and *s*-resonance spectra. In general, one axis is always more sensitive than the other, which means that the ratio of shifts on the *s*- and *p*-axes (i.e., the sensitivity factor, S_f) generated by the same amount of mass will be different from 1 (S_f equals 1 only for an ideal situation when both axes have the same sensitivity). Therefore, by taking into account the sensitivities of the *p*- and *s*-axes, one is able to place a mass axis into the coordinate system, i.e., to insert a line on which $\Delta s/\Delta p = S_f$. Furthermore, as noted in the previous section, because the mass changes cause the same directional alterations on both the *s*- and *p*-axes (i.e., either positive or negative shifts), the mass axis has to be placed in either the first or the third quadrants of the (*s*-*p*) coordinate system.
2. The optical symmetry of the measured system, i.e., whether the system is optically isotropic or anisotropic. For an anisotropic system, one must assume the direction of the optical axis, i.e., whether the optical axis is parallel to the *p*- or *s*-polarization direction. For an optical axis parallel to the *p*-direction, and a system containing elongated, rod-shaped molecules with their long molecular axis parallel to the optical axis of the system, the structural axis must be placed within the (*s*-*p*) coordinate system to fulfill the relationship: $2\,|\Delta s|/|\Delta p| = S_f$, whereas for an optical axis parallel to the *s*-direction the following relationship should be fulfilled: $|\Delta s|/2|\Delta p| = S_f$. Note that the factor of 2 that appears in these relations is due to the fact that in a deposited film the plane in which *s*-polarized changes occur is two-dimensional. Furthermore, as noted in the previous section, structural changes along the *p*-axis are always compensated by opposite changes in the *s*-plane, so that the total mass remains constant. Thus, in contrast to spectral shifts due to mass changes that occur in the same direction for both *s*- and *p*-polarized spectra, any alterations in anisotropy of the system produce shifts in opposite directions (i.e., if the *p*-component is shifted to positive values, the *s*-component shifts to negative values). This requires that the structural axis be placed in either the second or the fourth quadrants.

The axes of a new (mass/structure) coordinate system can be then scaled using the original (*s*/*p*) coordinates. Each point on the mass axis (Δ_m) can be expressed by changes of the original coordinates (Δs) and (Δp) as

$$\Delta_m = [(\Delta s)_m^2 + (\Delta p)_m^2]^{1/2}, \quad (1)$$

and on the structural axis,

$$\Delta_{str} = [(\Delta s)^2_{str} + (\Delta p)^2_{str}]^{1/2}. \quad (2)$$

In this way the contribution of structural changes and mass alterations are expressed in terms of angular shifts.

In the experimental example described below we have studied the interaction between a small cell-penetrating peptide (penetratin) and supported lipid membranes (Salamon et al., 2003), and have carried out simultaneous PWR and electrical impedance spectroscopy measurements of the system. A description of the experimental methods including cell design, formation of the solid-supported lipid bilayer, and PWR and impedance spectroscopy can be found in the earlier publication (Salamon et al., 2003). In this earlier article, both optical and electrical measurements included a full analysis involving spectral fitting. Here we intend to use some of these results in a graphical analysis procedure and to compare the results with the conclusions drawn in the previous publication. As will be demonstrated, the graphical procedure allows many of the same conclusions to be obtained in a much simpler manner.

RESULTS AND DISCUSSION

The experimental results obtained with lipid membranes interacting with penetratin (Salamon et al., 2003) have been acquired using a sensor characterized by a greater sensitivity with *p*-polarized light than with *s*-polarized light. In this system, the sensitivity factor is $S_f = \Delta s/\Delta p = 0.8$, i.e., for every 100-mdeg shift in the *p*-polarized spectrum there will be an 80-mdeg shift in the *s*-polarized spectrum, caused by any isotropic mass deposited on the surface of the sensor. Therefore, the mass axis that defines a set of points representing pure mass changes (i.e., without any contribution from structure or conformation changes) will be tilted away from the 45° line (where it would be when both axes are scaled the same), closer to the *p*-axis.

As has been described elsewhere, structural alterations defined by changes in both molecular orientation and conformation can be monitored by measuring the refractive index anisotropy (Salamon and Tollin, 2001a,b; Salamon et al., 2000a,b, 2003). This is an especially effective and useful approach with highly optically anisotropic, ordered molecular arrays consisting of elongated (rod-like) molecules, of which lipid bilayer membranes are a natural and very good example. Such systems are characterized by long-range ordering with an optical axis that is perpendicular to the surface of the membrane. Under the experimental conditions employed in PWR measurements, this axis can be approximated to be parallel to the electric vector of the *p*-polarized light used to excite the PWR spectra (Salamon et al., 1997). Thus, as noted above, the structural axis should be placed within the (*s*-*p*) coordinate system to fulfill the relationship: $2\,|\Delta s|/|\Delta p| = S_f$.

Taking the abovementioned principles into account, one is able to create a (mass-structure) coordinate system within the experimental (*s*-*p*) coordinate system. Furthermore, as indicated by Eqs. 1 and 2, the (mass-structure) axis can be scaled in mdeg using the original (*s*-*p*) axis scaling. It is also possible to scale the mass axis in absolute terms by calibrating the PWR instrument by binding a known quantity of material to the resonator surface, although this is not done in the following example. In this way, any experimental point which is originally derived from *s*- and *p*-polarized spectral shifts can be transformed into a (mass-structure) coordinate system, which allows one to separate the total spectral shifts into those caused by mass changes and those caused by structural changes.

It is important in the context of this discussion to clearly distinguish between the concepts of mass in the spectral fitting and graphical analysis procedures to compare results obtained by these two techniques. As noted above, PWR spectral shifts depend on both the amount of mass deposited per unit surface area as well as the way in which the mass is distributed along the *s*- and *p*-axes, i.e., the internal organization (or structure) of the molecules forming the deposited film. As has been discussed elsewhere (Salamon and Tollin, 2001b), the mass per unit surface area is proportional to both the square of the average refractive index and to the thickness of the film. Both of these parameters can be obtained individually from the spectral fitting method of analyzing the PWR data, and therefore the deposited mass can be directly calculated from those parameters. On the other hand, the graphical analysis procedure based on spectral shifts produces a single value representing mass per unit surface area, i.e., the mass shift values contain changes in both the square of the average refractive index and in the thickness. Therefore, to compare the mass changes obtained graphically with those obtained using the fitting parameters, one has to calculate mass changes in the latter procedure using both refractive indices and thickness to obtain the amount of deposited mass.

Furthermore, the refractive index can in general have different values in different directions (i.e., parallel or perpendicular to the surface). Such an optical anisotropy (or birefringence), resulting from the asymmetry in the molecular polarizability, long-range molecular orientation, and molecular shape of the deposited molecules (Salamon and Tollin, 2001a,b), is measured by the refractive index anisotropy as calculated from the individual refractive indices obtained in the spectral fitting technique, and describes the molecular arrangement (or structure) of the deposited material. The structural axis in the graphical analysis is defined so as to describe the changes in refractive index anisotropy produced by elongated molecules arranged with their long axes in a preferred direction. Therefore, any alteration in either molecular long-range orientation or molecular shape will result in changes of refractive index anisotropy and will be indicated by changes occurring on the structural axis. Thus,

there is a direct relationship between the refractive index anisotropy obtained from the spectral fitting procedure and employed in our previous publications, and the changes measured on the structural axis in the graphical analysis.

Fig. 1 illustrates this process by using the shift of the PWR spectra caused by deposition of an egg phosphatidylcholine bilayer (*BLM*) onto the sensor surface, compared to the spectral position of the resonance obtained from the bare sensor surface. The results used here were taken from Fig. 3 of Salamon et al. (2003) and were obtained using a PWR sensor with an indium tin oxide coating, a modification that allowed impedance measurements to be carried out. Note that the BLM spectrum is shifted by ~138 mdeg for *p*-polarized light and ~73 mdeg for *s*-polarized light, from the position of the bare sensor spectrum, which is plotted at the origin. These *p*- and *s*-coordinate values position the BLM point on the (*s*-*p*) graph presented in Fig. 1. From the positions of the mass and structure axes, one can evaluate the coordinates of this point relative to the (mass-structure) coordinate system, given by $\Delta p_m = 107$ mdeg; $\Delta s_m = 85$ mdeg; $\Delta p_{str} = 29$ mdeg; and $\Delta s_{str} = -11$ mdeg, as shown in Fig. 1. Then, using Eqs. 1 and 2, one can calculate values for a pure mass effect ($\Delta_m = 137$ mdeg) and a pure structural effect ($\Delta_{str} = 31$ mdeg), indicating that structural changes account for ~18% of the spectral changes whereas mass alterations account for ~82%. Furthermore, because the BLM point is located in the first quadrant of the (mass-structure) coordinate system, both mass and structural changes occur along the positive directions of the mass and structure axis, indicating that these changes result in increased values of mass and optical anisotropy. This result demonstrates that deposition of a lipid membrane not only increases the mass accumulated on the sensor surface, but also clearly shows that this mass is arranged in such a way that the refractive index along the optical axis (perpendicular to the sensor surface) increases. This observation is in good agreement with lipid bilayer optical properties. It is important to point out here that processes that generate a decrease of both mass and optical anisotropy will place the spectral shifts within the third quadrant. Similarly, the second quadrant will contain spectral shifts that result in a decrease of mass and an increase of anisotropy, whereas mass increases and refractive index anisotropy decreases will appear in the fourth quadrant. In this way, considerable insight can be obtained into the processes occurring in the deposited film, without the need for the complex numerical calculations involved in spectral curve fitting.

As has been demonstrated in our previous article (Salamon et al., 2003), addition of penetratin to the PWR sample compartment containing a deposited BLM caused further changes in the PWR spectra, including alterations in spectral position. Furthermore, the interaction between penetratin and the lipid membrane was very sensitive to the lipid composition, i.e., spectral changes obtained with a lipid membrane composed of egg phosphatidylcholine (PC) were much different in both the peptide concentration range in which they occurred, as well as the type of spectral changes produced, than those obtained with a mixture of 75 mol % egg PC + 25 mol % palmitoyloleoyl phosphatidylglycerol (POPG). Note that the latter BLM carries a net-negative charge and penetratin is a net-positively charged peptide. PWR spectral changes occurring after addition of aliquots of peptide solution into the aqueous compartment of the sample cell containing a preformed lipid bilayer membrane made with either of these two lipid compositions are illustrated in Fig. 2, *A* and *B*, by plotting the shifts in the angular position of the resonance spectra, obtained with both *p*- and *s*-polarized exciting light.

As we pointed out in the previous study (Salamon et al., 2003), the PWR results in Fig. 2 clearly indicate significant differences between the two lipid membranes in their

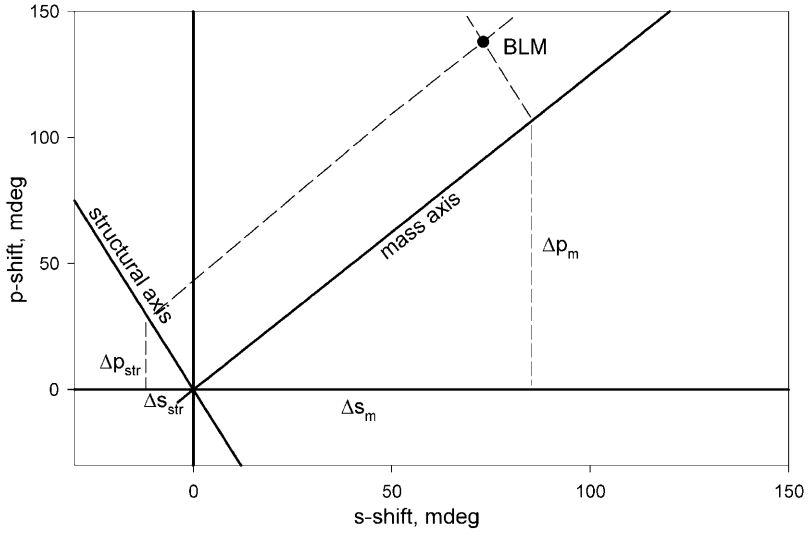

FIGURE 1 The PWR spectral position of an egg PC bilayer (*BLM*) formed with 20 mg/mL of egg PC dissolved in butanol containing 2.5% squalene within both (*s*-*p*) and (mass-structure) coordinate systems, obtained using a PWR sensor containing both SiO_2 and ITO layers as described in Salamon et al. (2003). (Δs_m), (Δp_m) and (Δs_{str}), (Δp_{str}) are the *s*- and *p*-coordinates describing either the mass shift or the structural shift caused by the BLM, respectively (see Eqs. 1 and 2).

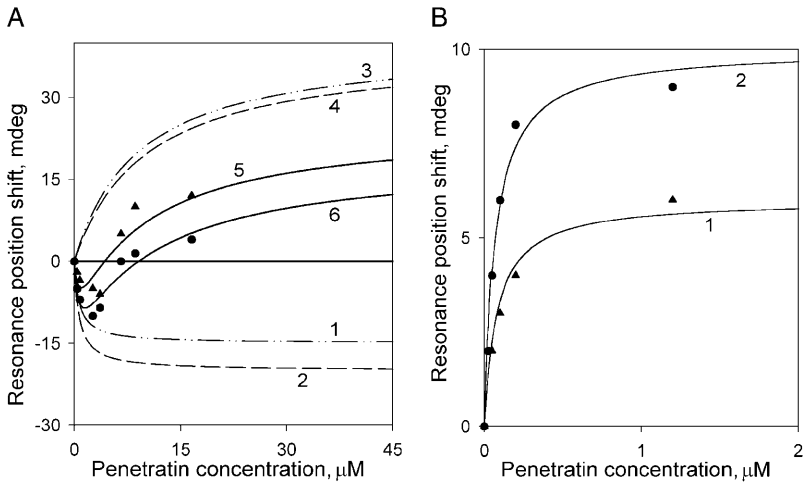

FIGURE 2 The PWR spectral maximum position shift (negative values represent a shift to smaller resonance angles) as a function of the concentration of added penetratin, obtained with the lipid membrane described in Fig. 1 *A* or an egg PC (75 mol %) + POPG (25 mol %) membrane (Fig. 1 *B*), using *p*- (●) or *s*-polarized (▲) light excitation (experimental data taken from Salamon et al., 2003). (*A*) Curves 1–4 represent the hyperbolic deconvolution of the experimental results: curves 1 (binding constant $k_D = 0.7 \pm 0.2\ \mu M$) and 3 ($k_D = 9 \pm 1\ \mu M$) for *s*-polarized spectra and curves 2 ($k_D = 0.7 \pm 0.2\ \mu M$) and 4 ($k_D = 10 \pm 1\ \mu M$) for the *p*-polarized spectra. Curve 5 is a sum of curves 1 and 3, whereas curve 6 is a sum of curves 2 and 4. (*B*) Curve 1 ($k_D = 0.08 \pm 0.02\ \mu M$) and curve 2 ($k_D = 0.07 \pm 0.02\ \mu M$) are the hyperbolic fits of the experimental resonance shifts obtained either with *s*- or with *p*-polarized light, respectively.

interaction with penetratin. First, the PC membrane shows a biphasic pattern of resonance shifts (initially shifting to smaller and then to larger angles), in contrast with the PC+POPG membrane that yields a simple hyperbolic concentration dependence curve. Second, the interaction between the lipid membrane and the peptide is shifted toward significantly higher penetratin concentrations for the PC membrane as compared with the PC+POPG bilayer, as expected from electrostatic considerations. Deconvolution of the spectral shifts obtained with the PC membrane (Fig. 2 *A*) leads to two hyperbolic curves in opposite direction for each polarization (*curves 1* and *3* for *s*-polarization; *curves 2* and *4* for *p*-polarization). Curve 5 is the sum of curves 1 and 3, whereas curve 6 is the sum of curves 2 and 4. The sum of the deconvoluted curves fit the experimental data points reasonably well. It is clear that curves 1 and 2 have similar penetratin concentration dependencies, with a binding constant of 0.7 μM for both *s*-and *p*-polarized spectra, and curves 3 and 4 describe another process, with binding constants equal to 9 and 10 μM for *s*- and *p*-polarization, respectively. These two pairs of hyperbolic curves can be used for graphical analysis of these two different processes. In contrast to the PC results, the data obtained with PC+POPG can be fit by a single pair of hyperbolic curves (Fig. 2 *B*), which also can be subjected to graphical analysis.

Fig. 3 shows a plot of the *s*- and *p*-spectral shifts on an (*s-p*) coordinate system, compared with the position of the BLM spectrum (the BLM point from Fig. 1 is now placed at the origin) for each of the two sets of deconvoluted hyperbolic curves from Fig. 2 *A* for the PC membrane (*open* and *solid circles*), for one set of hyperbolic curves from Fig. 2 *B* for the PC+POPG bilayer (*open triangles*), and for the actual experimental data for PC (*solid squares*) and PC+POPG (*solid triangles*). In general, any deviation from linearity between *s*- and *p*-shifts, as is especially apparent with the experimental results obtained with the PC membrane, is a clear indication that more than one process is responsible for such shifts. Furthermore, each point on the

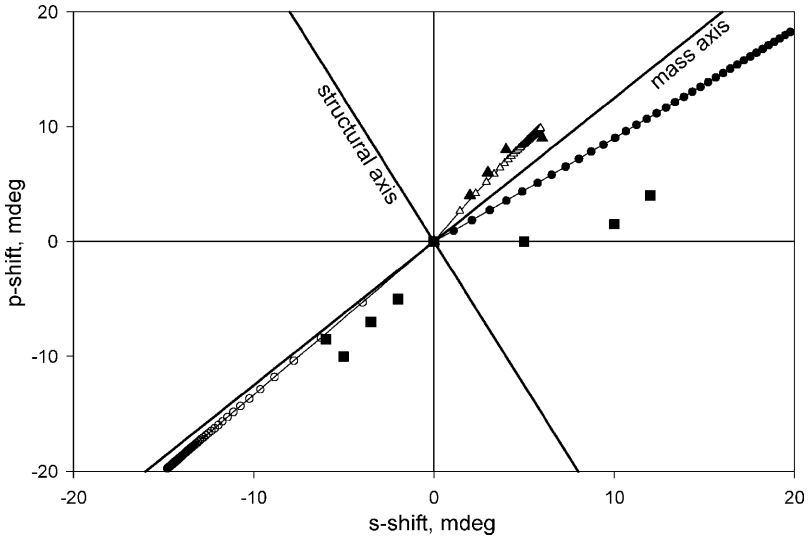

FIGURE 3 The PWR spectral position shifts shown in Fig. 2 are presented in the (*s-p*) and (mass-structure) coordinate systems for the experimental data (■, PC membrane; ▲, PC+POPG bilayer), and for the deconvoluted pairs of curves obtained either with the PC membrane (●, curves 3 and 4; ○, curves 1 and 2) or with the PC+POPG bilayer (△, curves 1 and 2).

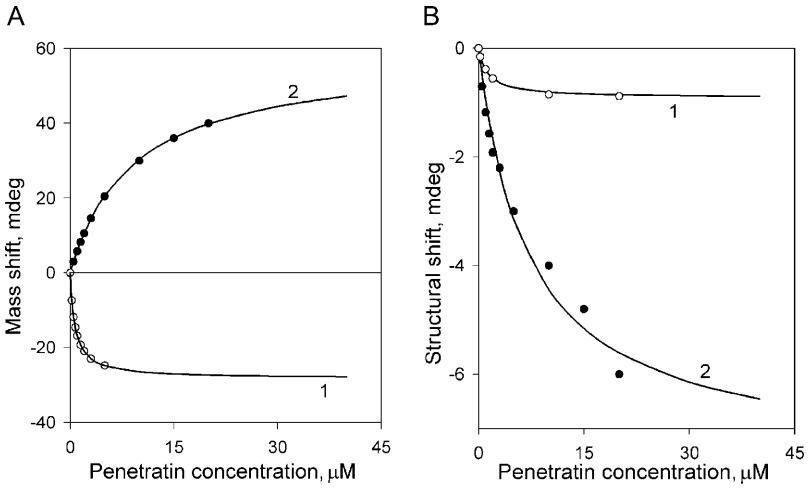

FIGURE 4 (*A*) Mass shifts as a function of penetratin concentration obtained with an egg PC membrane for the two binding processes, using either the ● (*curve 2*) or ○ (*curve 1*) data in Fig. 3, respectively. (*B*) Structural shifts as a function of penetration concentration obtained with an egg PC membrane for the same data as described in *A*. Data points shown in both *A* and *B* represent calculated mass and structural shifts using Fig. 3 and Eqs. 1 and 2; the curves are the hyperbolic fits to these calculated points. The percentages of the total shifts due to mass changes and structural changes calculated at 40-μM peptide concentration for the two processes are as follows: tight binding process corresponds to 97% mass and 3% structure; weaker binding process corresponds to 88% mass and 12% structure.

(*s-p*) coordinate system is obtained for a specific peptide concentration and can be transformed into the (mass-structure) coordinate system, which allows a separation of shifts caused by mass changes from those caused by structural changes (see Fig. 1). The concentration dependences of the calculated mass and structural effects are shown in Figs. 4 and 6 for the PC and PC+POPG lipid membranes, respectively.

In this context, it should be noted that positive shifts result from an increase of mass and refractive index anisotropy (Salamon et al., 2003), whereas negative shifts correspond to a decrease of mass and anisotropy. This allows us to qualitatively compare the results obtained here using the graphical approach with those derived previously using the spectral fitting procedure. For the simple situation when only one type of process is producing changes in the PWR spectra such comparison is direct and obvious. This is the case with the PC+POPG lipid membrane presented in Fig. 6, where only one pair of curves representing changes of mass and structure resulted from the graphic analysis. As can be seen, the results shown in Fig. 6 indicating an increase in mass and structural anisotropy are qualitatively very similar to those presented in Fig. 7 *B* of Salamon et al. (2003), obtained with considerably more time and effort using the fitting technique, which also reflect an increase in average refractive index and refractive index anisotropy, although without a significant change in film thickness.

In more complex cases where more than one process contributes to a final experimental shift, the graphical analysis allows a description of the changes in mass and structure created by each process, whereas the fitting procedure can only describe the final effect of mass and structure alterations resulting from all of the individual processes. In the latter case, therefore, the graphical analysis provides more insight into the mechanism than does the fitting method. Fig. 4 illustrates this point very well. Two pairs of curves are shown representing mass and structural changes for the two processes involved in the interaction between the PC membrane and penetratin. These two processes, as the graphical analysis clearly demonstrates, are distinguished by the magnitude of the binding constants, by the direction of the alteration in mass and by the magnitude of the structural change. Thus, the tighter binding process results in a decrease of both the mass and optical anisotropy, whereas the weaker binding process produces a decrease in the optical anisotropy and an increase in mass.

In this situation, it is important to recall that the mass described in the graphical analysis procedure represents not only changes in the average refractive index but also thickness changes as well, whereas in the spectral fitting method, these two quantities are individually obtained (Salamon et al., 2003). Thus, to directly compare the results presented in Fig. 4 with those previously obtained with the fitting technique, in which thickness changes were found to

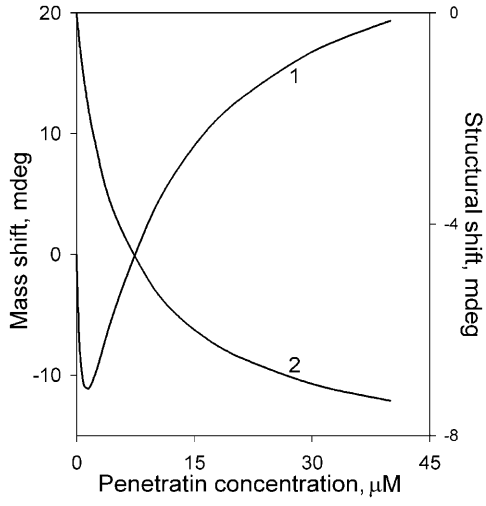

FIGURE 5 Plots of the sum of either the mass shift (*curve 1*) or the structural shift (*curve 2*) as a function of penetratin concentration, obtained using curves 1 and 2 from Fig. 4, *A* or *B*, respectively, for the two processes involved in binding.

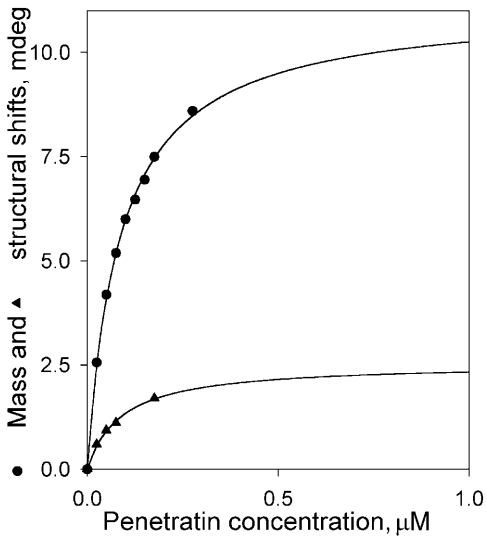

FIGURE 6 The mass and structural shifts as a function of penetratin concentration obtained with the PC+POPG membrane. Data points represent calculated mass and structural shifts using data from Fig. 3 and Eqs. 1 and 2; the curves are hyperbolic fits to these calculated points. The percentages of the total shifts due to mass changes and structural changes at 1-μM peptide concentration are 81% mass and 19% structure.

occur (Salamon et al., 2003), one has to sum the individual changes in the mass and structural effects for the two phases. The results of this summation are shown in Fig. 5. These are in good qualitative agreement with those presented in Fig. 6 of Salamon et al. (2003), where it was shown that the optical anisotropy decreases with increasing peptide concentration (compare with *curve 2* of Fig. 5 here), whereas the average refractive index also decreases but the thickness increases, which results in an overall increase of mass (compare with *curve 1* of Fig. 5 here). However, note that the graphical analysis shows that the mass increase is biphasic, which was not evident from the fitting results. This is an additional benefit of the graphical procedure.

CONCLUSIONS

The results presented here describe a graphical approach to analyzing spectral changes resulting from molecular interactions occurring within a thin film deposited on the surface of a PWR resonator. It is shown that data corresponding to spectral shifts in the *p*- and *s*-polarized resonances can be transformed into changes in mass per unit surface area (corresponding to the summation of average refractive index and film thickness) and structure (defined in terms of refractive index anisotropy). This provides a simpler and faster route to obtaining insights into the nature of the processes occurring in these films than is possible using the more tedious and time-consuming spectral fitting procedures. It should be kept in mind that the latter process allows absolute values to be individually obtained for these three parameters, whereas the graphical procedure expresses mass and structure in terms of spectral shift values, although it is possible to calibrate the shift scale by binding known amounts of material to the resonator surface thereby allowing an absolute determination of mass density changes. An additional advantage of the graphical method is that it allows a facile deconvolution of the pathway followed in producing mass and structure changes in systems in which a complex sequence of multiple events occurs; this cannot be accomplished using the spectral fitting procedure. We believe that this new methodology should be of particular benefit in experiments involving membrane-bound receptors, in which multiple conformations of the receptor exist whose populations are selectively and differentially altered by the binding of various types of ligands (Salamon et al., 2002, 2000a). This will be illustrated in subsequent publications.

The authors acknowledge Drs. Glen Ramsay and Vladimir Razinkov of Proterion Corporation for suggesting using pictorial representations of PWR spectral shifts for data analysis.

This work was supported by a grant from the National Institutes of Health (GM59630).

REFERENCES

Salamon, Z., M. F. Brown, and G. Tollin. 1999. Plasmon resonance spectroscopy: probing interactions within membranes. *Trends Biochem. Sci.* 24:213–219.

Salamon, Z., S. Cowell, E. Varga, H. I. Yamamura, V. J. Hruby, and G. Tollin. 2000a. Plasmon resonance studies of agonist/antagonist binding to the human δ-opioid receptor: new structural insight into receptor-ligand interactions. *Biophys. J.* 79:2463–2474.

Salamon, Z., J. T. Hazzard, and G. Tollin. 1993. Direct measurement of cyclic current-voltage responses of integral membrane proteins at a self-assembled lipid-bilayer-modified electrode: cytochrome f and cytochrome c oxidase. *Proc. Natl. Acad. Sci. USA.* 90:6420–6423.

Salamon, Z., V. J. Hruby, G. Tollin, and S. Cowell. 2002. Binding of agonists, antagonists and inverse agonist to the human δ-opioid receptor produces distinctly different conformational states distinguishable by plasmon-waveguide resonance spectroscopy. *J. Pept. Res.* 60:322–328.

Salamon, Z., G. Lindblom, L. Rilfors, K. Linde, and G. Tollin. 2000b. Interaction of phosphatidylserine synthase from *E. coli* with lipid bilayers: coupled plasmon-waveguide resonance spectroscopy studies. *Biophys. J.* 78:1400–1412.

Salamon, Z., G. Lindblom, and G. Tollin. 2003. Plasmon-waveguide resonance and impedance spectroscopy studies of the interaction between penetratin and supported lipid bilayer membranes. *Biophys. J.* 84: 1796–1807.

Salamon, Z., H. A. Macleod, and G. Tollin. 1997. Coupled plasmon-waveguide resonators: a new spectroscopic tool for probing proteolipid film structure and properties. *Biophys. J.* 73:2791–2797.

Salamon, Z., and G. Tollin. 1999a. Surface plasmon resonance, theory. *In* Encyclopedia of Spectroscopy and Spectrometry, Vol. 3. J. C. Lindon, G. E. Tranter, and J. L. Holmes, editors. Academic Press, New York. 2311–2319.

Salamon, Z., and G. Tollin. 1999b. Surface plasmon resonance, applications. *In* Encyclopedia of Spectroscopy and Spectrometry, Vol. 3. J. C. Lindon, G. E. Tranter, and J. L. Holmes, editors. Academic Press, New York. 2294–2302.

Salamon, Z., and G. Tollin. 2000. Surface plasmon resonance spectroscopy in peptide and protein analysis. *In* Encyclopedia of Analytical Chemistry.

R. A. Meyers, editor. John Wiley and Sons, Chichester, England. 6050–6061.

Salamon, Z., and G. Tollin. 2001a. Plasmon resonance spectroscopy: probing molecular interactions at surfaces and interfaces. *Spectroscopy*. 15:161–175.

Salamon, Z., and G. Tollin. 2001b. Optical anisotropy in lipid bilayer membranes: coupled plasmon-waveguide resonance measurements of molecular orientation, polarizability, and shape. *Biophys. J.* 80:1557–1567.

Salamon, Z., Y. Wang, G. Tollin, and H. A. Macleod. 1994. Assembly and molecular organization of self-assembled lipid bilayers on solid substrates monitored by surface plasmon resonance spectroscopy. *Biochim. Biophys. Acta*. 1195:267–275.